

JUL 14 1988

NBSIR 88-3734

Estimating the Environment and the Response of Sprinkler Links in Compartment Fires with Draft Curtains and Fusible Link-Actuated Ceiling Vents - Part I: Theory

Leonard Y. Cooper

U.S. DEPARTMENT OF COMMERCE
National Bureau of Standards
National Engineering Laboratory
Center for Fire Research
Gaithersburg, MD 20899

April 1988

Sponsored by:

AAMA Research Foundation
2700 River Road, Suite 118
Des Plaines, Illinois 60018



75 Years Stimulating America's Progress
1913-1988

NBSIR 88-3734

**ESTIMATING THE ENVIRONMENT
AND THE RESPONSE OF SPRINKLER
LINKS IN COMPARTMENT FIRES WITH
DRAFT CURTAINS AND FUSIBLE
LINK- ACTUATED CEILING VENTS -
PART I: THEORY**

Leonard Y. Cooper

U.S. DEPARTMENT OF COMMERCE
National Bureau of Standards
National Engineering Laboratory
Center for Fire Research
Gaithersburg, MD 20899

April 1988

Sponsored by:
AAMA Research Foundation
2700 River Road, Suite 118
Des Plaines, Illinois 60018



U.S. DEPARTMENT OF COMMERCE, C. William Verity, *Secretary*
NATIONAL BUREAU OF STANDARDS, Ernest Ambler, *Director*

TABLE OF CONTENTS

	<u>Page</u>
LIST OF FIGURES	iv
ABSTRACT	1
1. Introduction	2
2. The Basic Equations	2
3. Mass Flow and Enthalpy Flow Plus Heat Transfer	5
3.1. Flow to the Upper Layer from the Vents	5
3.2. Flow to the Layer from the Plume and Radiation from the Fire	5
3.3. Flow to the Layer from Below the Curtains	7
3.4. Heat Transfer to the Upper Layer	8
3.4.1. Properties of the Plume in the Upper Layer When $y_{\text{FIRE}} < y$	8
3.4.2. General Properties of the Plume in the Upper Layer	11
3.4.3. Computing q_{HT} and the Thermal Response of the Ceiling	11
3.4.3.1. Net Heat Transfer Flux to the Ceiling's Lower Surface	13
3.4.3.2. Net Heat Transfer Flux to Ceiling's Upper Surface	14
3.4.3.3. Solving for the Thermal Response of the Ceiling and for q_{HT}	15
4. Actuation of Vents and Sprinklers by Near-Ceiling-Deployed Fusible Links	16
4.1 Predicting the Thermal Response of the Fusible Links	16
4.2 The Velocity Distribution of the Ceiling Jet	17
4.3 The Temperature Distribution of the Ceiling Jet	18
4.4 Dependence of Open Vent Area on Fusible Link-Actuated Vents	20
5. Initiating the Solution of the Model Equations	21
6. Concluding Remarks	22
7. Acknowledgements	22
8. References	23
9. Nomenclature	25

LIST OF FIGURES

	<u>Page</u>
Figure 1. Fire in a building space with draft curtains and ceiling vents	29
Figure 2. The fire and the equivalent source in the lower layer and the continuation source in the extended upper layer	30
Figure 3. A plot of dimensionless ceiling jet velocity distribution, V_{CJ}/V_{MAX} , as a function of $z/(0.23\delta)$ per Eq. (49)	31
Figure 4. Plots of dimensionless ceiling jet temperature distribution, θ , as a function of $z/(0.23\delta)$ per Eq. (52) for cases when θ_s is < 0 , between 0 and 1, and > 0	32

ESTIMATING THE ENVIRONMENT AND THE RESPONSE OF SPRINKLER LINKS IN
COMPARTMENT FIRES WITH DRAFT CURTAINS AND FUSIBLE LINK-ACTUATED
CEILING VENTS - PART I: THEORY

Leonard Y. Cooper

ABSTRACT

The physical basis and associated mathematical model for estimating the fire-generated environment and the response of sprinkler links in well-ventilated compartment fires with draft curtains and fusible link-actuated ceiling vents is developed. Complete equations and assumptions are presented. Phenomena taken into account include: the flow dynamics of the upward-driven, buoyant fire plume; growth of the elevated-temperature smoke layer in the curtained compartment; the flow of smoke from the layer to the outside through open ceiling vents; the flow of smoke below curtain partitions to building spaces adjacent to the curtained space of fire origin; continuation of the fire plume in the upper layer; heat transfer to the ceiling surface and the thermal response of the ceiling as a function of radial distance from the point of plume-ceiling impingement; the velocity and temperature distribution of plume-driven near-ceiling flows and the response of near-ceiling-deployed fusible links as functions of distance below the ceiling and distance from plume-ceiling impingement.

The theory presented here is the basis of a computer model now under development which will be used to study parametrically a wide range of relevant fire scenarios. The results of the parametric study will be presented in the Part II: Applications portion of this paper.

Keywords: algorithms; building fires; compartment fires; computer models; fire models; mathematical models; vents; sprinkler response; zone models.

1. Introduction

Consider a space of plan area A defined by ceiling-mounted draft curtains with a fire of time-dependent energy release rate $Q(t) > 0$ and with open ceiling vents of total time-dependent area $A_v(t)$. The curtained area can be considered as one of several such spaces in a large building compartment. Also, by specifying the curtains to be deep enough they can be thought of as simulating the walls of a single uncurtained compartment. This paper presents the physical basis and associated mathematical model for estimating the fire-generated environment and the response of sprinkler links in curtained compartment fires with fusible link-actuated ceiling vents. The problem addressed in this work is similar to the problem addressed in [1]. The theory presented here is the basis of a computer model which will be developed and then used to study parametrically a wide range of relevant fire scenarios. The results of the parametric study will be presented in the Part II: Applications portion of this paper [2].

The overall building compartment is assumed to have near-floor wall vents which are large enough to maintain the inside environment, below any near-ceiling smoke layers which may form, at assumed initial outside-ambient conditions. Figure 1 depicts the generic fire scenario of interest. The assumption of large near-floor wall vents will require that the modeling be restricted to conditions where y , the elevation of the smoke layer interface, is above the floor elevation, i.e., $y > 0$. The assumption also has important implications with regard to the cross-ceiling vent pressure differential. This is the pressure differential which drives elevated-temperature upper layer smoke through the ceiling vents to the outside. Thus, below the smoke layer (i.e., from the floor of the facility to the elevation of the smoke layer interface) the inside-to-outside hydrostatic pressure differential will be zero, while a positive inside-to-outside pressure differential will exist at all elevations in the reduced-density smoke layer itself (higher pressure inside the curtained area, lower pressure in the outside environment), the maximum differential occurring at the ceiling and across the open ceiling vents.

2. The Basic Equations

A two-layer zone-type compartment fire model is used to describe the phenomena under investigation and, as is typical in such models, the upper smoke layer is assumed to be uniform in density, ρ_U , and absolute temperature, T_U . The following time-dependent equations describe conservation of energy, mass and the perfect gas law in the upper smoke layer

Conservation of Energy:

$$d[(y_{CEIL} - y)\rho_U T_U A C_v]/dt = q_U + p A dy/dt \quad (1)$$

Conservation of Mass:

$$d[(y_{CEIL} - y)\rho_U A]/dt = m_U \quad (2)$$

Perfect Gas Law:

$$p_U/R = p/R = \text{constant} = \rho_U T_U = \rho_{AMB} T_{AMB}, \text{ i.e., } T_U = T_{AMB} (\rho_{AMB}/\rho_U) \quad (3)$$

where y_{CEIL} is the elevation of the ceiling above the floor, $R = C_p - C_v$ is the gas constant, C_p and C_v are the specific heats at constant pressure and volume, respectively, and p is a constant characteristic pressure, say, p_{ATM} at the floor elevation. In Eq. (1) q_U is the net rate of enthalpy flow plus heat transfer to the upper layer and is made up of flow components: q_{CURT} , from below the curtain, q_{PLUME} , from the plume, q_{VENT} , from the ceiling vent; and the component q_{HT} , the total heat transfer rate

$$q_U = q_{CURT} + q_{PLUME} + q_{VENT} + q_{HT} \quad (4)$$

In Eq.(2) m_U is the net rate of mass flow to the upper layer with flow components: m_{CURT} , from below the curtain, m_{PLUME} , from the plume, and m_{VENT} , from the ceiling vent

$$m_U = m_{CURT} + m_{PLUME} + m_{VENT} \quad (5)$$

Using Eq. (3) in Eq. (1) leads to

$$dy/dt = - q_U / (A C_p \rho_{AMB} T_{AMB}) \quad (6)$$

if ($y = y_{CEIL}$ and $q_U \geq 0$) or ($0 < y < y_{CEIL}$ and arbitrary q_U)

The first of these conditions will be seen below to be consistent with our earlier, $Q > 0$ assumption. In particular, we will see that $q_U > 0$ initially when $y = y_{CEIL}$. Therefore, Eq. (6) will always be applicable.

Using Eq.(1), Eq. (2) can be rewritten as

$$d\rho_U/dt = (m_U + \rho_U A dy/dt) / [(y_{CEIL} - y)A] \text{ if } 0 < y < y_{CEIL} \quad (7)$$

Since the denominator of Eq. (7) is zero at the initiation of a fire (i.e., when $y=y_{\text{CEIL}}$), $d\rho_U/dt$ is indeterminate at that time. However, as mentioned above, in our $Q>0$ scenarios $q_U>0$ generally at $t=0$ and for this reason a non-zero, initial dy/dt value is predicted by Eq. (6). Then, since $d\rho_U/dt$ of Eq. (7) is expected to exist for $t>0$ it is reasonable to require the numerator of Eq. (7) to be zero at $t=0$, thereby obtaining the initial value of ρ_U . Doing this leads to

$$\rho_U(t = 0) = \rho_{\text{AMB}} T_{\text{AMB}} C_p m_U / q_U \quad (8)$$

The above value for $\rho_U(t=0)$ can be shown to be identical to the initial average density of the plume flow at the elevation of ceiling impingement after all heat transfer from the plume-flow-driven ceiling and wall jets have been taken into account.

Solving for ρ_U requires a definite value for $d\rho_U/dt$ at $t=0$, i.e., at $y=y_{\text{CEIL}}$, which is not provided in Eq. (7). To obtain the correct value for this requires the results of a detailed analysis of the limiting small- t values of m_U , dm_U/dt , q_U , and dq_U/dt . Such an analysis can only be carried out within the context of a specific plume model. To avoid this problem, we will take arbitrarily the value of $d\rho_U/dt$ to be zero at $t=0$. Thus, Eq. (7) becomes

$$d\rho_U/dt = \begin{cases} (m_U + \rho_U A dy/dt) / [(y_{\text{CEIL}} - y)A] & \text{if } 0 < y < y_{\text{CEIL}} \\ 0 & \text{if } t = 0, \text{ i.e., when } y = y_{\text{CEIL}} \end{cases} \quad (7')$$

it is expected that by using a robust numerical integrator and relatively tight tolerances to solve the governing Eqs. (6) and (7') the solution for ρ_U will recover quickly from an incorrect initial value for $d\rho_U/dt$ and the correct solution for ρ_U will still be obtained for $t>0$.

The basic problem of simulating mathematically the growth and properties of the upper layer for the generic Figure 1 scenario will require the solution of the system of Eqs. (6) and (7') for y and ρ_U . Using the computed values of ρ_U at any instant of time, the subsidiary Eq. (3) can then be used to solve for T_U . To integrate Eqs. (6) and (7') requires algorithms for calculating the various components of q_U and m_U indicated in Eqs. (4) and (5). These will be obtained below.

3. Mass Flow and Enthalpy Flow Plus Heat Transfer

3.1. Flow to the Upper Layer from the Vents

Conservation of momentum across all open ceiling vents as expressed by Bernoulli's equation leads to

$$V = C(2\Delta P_{CEIL}/\rho_U)^{1/2} \quad (9)$$

$$m_{VENT} = -\rho_U A_V V = -A_V C(2\rho_U \Delta P_{CEIL})^{1/2} \quad (10)$$

where V is the average velocity through all open vents, C is the vent flow coefficient (≈ 0.68 [3]), and ΔP_{CEIL} is the cross-vent pressure difference.

From hydrostatics

$$\Delta P_{CEIL} \equiv P_U(y=y_{CEIL}) - P_{AMB}(y=y_{CEIL}) = (\rho_{AMB} - \rho_U)g(y_{CEIL} - y) \quad (11)$$

where g is the acceleration of gravity.

Substituting Eq. (11) in Eq.(10) leads to the desired result for m_{VENT}

$$m_{VENT} = -A_V C[2\rho_U(\rho_{AMB} - \rho_U)g(y_{CEIL} - y)]^{1/2} \quad (12)$$

which is equivalent to the equations used to estimate ceiling vent flow rates in [4] and [5]. Using Eq. (12) we can obtain the desired result for q_{VENT}

$$q_{VENT} = m_{VENT} C_p T_U \quad (13)$$

3.2. Flow to the Layer from the Plume and Radiation from the Fire

It is assumed that the mass generation rate of the fire is small compared to m_{ENT} , the rate of mass of air entrained into the plume between the fire elevation, y_{FIRE} , and the layer interface, or compared to other mass flow rate components of m_U . It is also assumed that all of the m_{ENT} penetrates the layer interface and enters the upper layer. Thus

$$m_{\text{PLUME}} = m_{\text{ENT}} \quad (14)$$

and

$$q_{\text{PLUME}} = m_{\text{ENT}} C_p T_{\text{AMB}} + (1 - \lambda_r) Q \quad (15)$$

The first term on the right side of Eq. (15) is the enthalpy associated with m_{ENT} and λ_r of the second term is the effective fraction of Q assumed to be radiated isotropically from the fire's combustion zone.

It is assumed that the smoke layer is relatively transparent and that it does not participate in any significant radiation heat transfer exchanges. In particular, all of the $\lambda_r Q$ radiation is assumed to be incident on the bounding surfaces of the compartment. Thus, the last term of Eq. (15) is the net amount of enthalpy added to the upper layer from the combustion zone and its buoyantly-driven plume. Flaming fires exhibit λ_r 's of $0 < \lambda_r < 0.6$, e.g., smaller values for small methane fires and the higher values for large polystyrene fires. However, for a hazardous fires involving a wide range of common groupings of combustibles, it is reasonable to approximate flame radiation by choosing $\lambda_r \approx 0.35$ [6].

A specific plume entrainment model is required to complete Eqs. (14)-(15) for m_{PLUME} and q_{PLUME} . The following estimate for m_{ENT} , developed in [7] and discussed in [8] will be adopted here

$$m_{\text{ENT}} / (\text{kg/s}) = \begin{cases} 0 & \text{if } y - y_{\text{FIRE}} \leq 0; \\ 0.0054[(1 - \lambda_r)(Q/kW)](y - y_{\text{FIRE}})/L_{\text{FLAME}} & \text{if } 0 < (y - y_{\text{FIRE}})/L_{\text{FLAME}} < 1; \\ 0.071[(1 - \lambda_r)(Q/kW)]^{1/3} \cdot \left\{ \begin{array}{l} (y - y_{\text{FIRE}} - L_{\text{FLAME}})/m + 0.166[(1 - \lambda_r)(Q/kW)]^{2/5} \end{array} \right\}^{5/3} \\ \quad \cdot \left[\begin{array}{l} 1 + \epsilon[(1 - \lambda_r)(Q/kW)]^{2/3} \\ \cdot \left\{ (y - y_{\text{FIRE}} - L_{\text{FLAME}})/m + 0.166[(1 - \lambda_r)(Q/kW)]^{2/5} \end{array} \right\}^{-5/3} \end{array} \right] & \text{if } (y - y_{\text{FIRE}})/L_{\text{FLAME}} \geq 1 \end{cases} \quad (16)$$

$$L_{\text{FLAME}}/D_{\text{FIRE}} = -1.02 + 0.249[(1 - \lambda_r)(Q/kW)]^{2/5}/(D_{\text{FIRE}}/m) \quad (17)$$

$$\epsilon = 0.0054/0.071 - (0.166)^{5/3} = 0.0259168209\dots \approx 0.026 \quad (18)$$

where L_{FLAME} is the fire's flame length, D_{FIRE} is the effective diameter of the fire source ($\pi D_{\text{FIRE}}^2/4 =$ area of the fire source), and ϵ is chosen so that, analytically, the value of m_{ENT} is exactly continuous at the elevation $y - y_{\text{FIRE}} = L_{\text{FLAME}}$.

3.3. Flow to the Layer from Below the Curtains

If the upper layer interface, y , drops below the elevation of the bottom of the curtains, y_{CURT} , then there will be mass and enthalpy flows from the upper layer of the curtained area where the fire is located to adjacent curtained areas of the overall building compartment. The mass flow rate will be the result of hydrostatic cross-curtain pressure differentials. Provided adjacent curtained areas are not yet filled with smoke, this pressure differences increases linearly from zero at the layer interface to Δp_{CURT} at $y = y_{\text{CURT}}$. From hydrostatics

$$\Delta p_{\text{CURT}} \equiv p_U(y = y_{\text{CURT}}) - p_{\text{AMB}}(y = y_{\text{CURT}}) = (\rho_{\text{AMB}} - \rho_U)g(y_{\text{CURT}} - y) \quad (19)$$

Using Eq. (19) together with well-known vent flow relations (e.g., Eq. (31) of [3]) m_{CURT} and the q_{CURT} can be estimated from

$$m_{\text{CURT}} = \begin{cases} 0 & \text{if } y \geq y_{\text{CURT}}; \\ -(L_{\text{CURT}}/3)[8(y_{\text{CURT}} - y)^3 \rho_U (\rho_{\text{AMB}} - \rho_U)g]^{1/2} & \text{if } y \leq y_{\text{CURT}} \end{cases} \quad (20)$$

$$q_{\text{CURT}} = m_{\text{CURT}} C_p T_U \quad (21)$$

where L_{CURT} is that length of the perimeter of area A which is connected to other curtained areas of the overall building compartment. For example, if the curtained area is in one corner of the building compartment, then the length of its two sides coincident with the walls of the compartment will not be included in L_{CURT} . Since the generic vent flow configuration under consideration here is very long and narrow, a flow coefficient for the vent flow used in Eq. (20) was taken to be 1.

3.4. Heat Transfer to the Upper Layer

As discussed above in section 3.2., when the fire is below the layer interface the buoyant fire plume rises toward the ceiling and all of its mass and enthalpy flow, m_{PLUME} and q_{PLUME} , is assumed to be deposited into the upper layer. Having penetrated the interface, the plume continues to rise toward the ceiling of the curtained compartment. As it impinges on the ceiling surface, the plume flow turns and forms a relatively high temperature, high velocity, turbulent ceiling jet which flows radially outward along the ceiling and transfers heat to the relatively cool ceiling surface. The ceiling jet is cooled by convection and the ceiling material is heated in depth by conduction. The convective heat transfer rate is a strong function of the radial distance from the point of plume/ceiling impingement, reducing rapidly with increasing radius. It is dependent also on the characteristics of the plume immediately upstream of ceiling impingement.

The ceiling jet is blocked eventually by the curtains and/or wall surfaces. It then turns downward and forms vertical surface flows. In the case of wall surfaces and very deep curtains, the descent of these flows is stopped eventually by upward buoyant forces and they mix finally with the upper layer. Here we assume that the plume/ceiling impingement point is relatively far from the closest curtain or wall surface, say, greater than a few fire-to-ceiling lengths. Under such circumstances the ceiling jet - wall flow interactions will be relatively weak and, compared to the net rate of heat transfer from the ceiling and near the plume/ceiling impingement point, the heat transfer to the upper layer from all vertical surfaces will be relatively small.

Define λ_{CONV} as the fraction of Q which is transferred by convection from the upper layer gas ceiling jet to the ceiling and wall/curtain surfaces

$$q_{\text{HT}} = -\lambda_{\text{CONV}}Q \quad (22)$$

Once the values of $\lambda_{\text{CONV}}Q$ and q_{HT} are determined from a time-dependent solution to the coupled, ceiling jet/ceiling material, convection/conduction problem the task of determining an estimate for each component of m_{U} and q_{U} will be complete.

3.4.1. Properties of the Plume in the Upper Layer When $y_{\text{FIRE}} < y$

Consider times when the elevation of the fire is below the interface, i.e., when $y_{\text{FIRE}} < y$.

As the plume flow enters the upper layer the forces of buoyancy which act to drive the plume toward the ceiling (i.e., as a result of relatively high-temperature, low-density plume gases being submerged in a relatively cool, high-density ambient environment) are reduced immediately because of the temperature increase of the upper layer environment over that of the lower

ambient. As a result, the continued ascent of the plume gases will be less vigorous, i.e., at reduced velocity, and of higher temperature than it would have been in the absence of the layer. Indeed, some of the penetrating plume flow, will actually be at a lower temperature than T_U . The upper layer buoyant forces on this latter portion of the flow will actually retard and possibly stop its subsequent rise to the ceiling.

The simple point source plume model of [9] will be used to simulate the plume flow, first immediately below, or upstream of the interface, and then throughout the depth of the upper layer itself.

The plume above a Reference-[9]-type point source of buoyancy, where the source is below the interface, will be equivalent to the plume of our fire (in the sense of having identical mass and enthalpy flow rates at the interface) if the point source strength is $(1-\lambda_r)Q$ and the elevation of the equivalent source, y_{EQ} , satisfies

$$m_{PLUME} = 0.21\rho_{AMB}g^{1/2}(y - y_{EQ})^{5/2}Q_{EQ}^{*1/3} \quad (23)$$

In the above, Q_{EQ}^* , a dimensionless measure of the strength of the fire plume at the interface, is defined as

$$Q_{EQ}^* = (1 - \lambda_r)Q/[\rho_{AMB}C_pT_{AMB}g^{1/2}(y - y_{EQ})^{5/2}] \quad (24)$$

Note that at an arbitrary instant of time in the simulation of a fire scenario, m_{PLUME} in Eq. (23) is a known value that would be determined previously from Eqs. (14) and (16).

Using (23) and (24) we solve for y_{EQ} and Q_{EQ}^*

$$y_{EQ} = y - [(1 - \lambda_r)Q/(Q_{EQ}^*\rho_{AMB}C_pT_{AMB}g^{1/2})]^{2/5} \quad (25)$$

$$Q_{EQ}^* = [0.21(1 - \lambda_r)Q/(C_pT_{AMB}m_{PLUME})]^{3/2} \quad (26)$$

Now as the plume crosses the interface, the fraction, m^* , of m_{PLUME} which is still buoyant relative to the upper layer environment and presumably continues to rise to the ceiling, entraining upper layer gases along the way, is predicted in [10] to be

$$m^* = \begin{cases} 0; & -1 < \sigma \leq 0 \\ (1.04599\sigma + 0.360391\sigma^2)/(1. + 1.37748\sigma + 0.360391\sigma^2) ; & \sigma > 0 \end{cases} \quad (27)$$

where the dimensionless parameter σ is defined as

$$\sigma = (1 - \alpha + C_T Q_{EQ}^{*2/3}) / (\alpha - 1) \quad (28)$$

$$\alpha = T_U / T_{AMB} ; C_T = 9.115 \quad (29)$$

and where Q_{EQ}^* is the value computed above in Eq. (26). Reference [10] identifies further the parameters necessary to describe plume flow continuation in the upper layer (i.e., between y and y_{CEIL}) according to a Reference-[9]-type point source plume. It has been determined that this plume can be modeled as being driven by a non-radiating buoyant source of strength Q' located a distance

$$H = y_{CEIL} - y'_{SOURCE} > y_{CEIL} - y_{FIRE} \quad (30)$$

below the ceiling in a (downward-) extended upper layer environment of temperature T_U and density ρ_U . The relevant parameters predicted in [10] are

$$Q' = (1 - \lambda_r) Q \sigma m^* / (1 + \sigma) \quad (31)$$

$$y'_{SOURCE} = y - (y - y_{EQ}) \alpha^{3/5} m^{*2/5} [(1 + \sigma) / \sigma]^{1/5} \quad (32)$$

The fire and the equivalent source in the lower layer and the continuation source in the upper layer are depicted in Figure 2. Times during a fire simulation when Eq. (28) predicts $\sigma \gg 1$ are related to states of the fire environment when the temperature distribution above T_{AMB} of the plume flow, at the elevation of interface penetration, is predicted to be mostly much larger than $(T_U - T_{AMB})$. Under such circumstances the penetrating plume flow is still very strongly buoyant as it enters the upper layer. The plume will continue to rise to the ceiling and to drive ceiling jet convective heat transfer at rates which differ only slightly (on account of the elevated temperature upper layer environment) from the heat transfer rates which could occur in the absence of an upper layer.

Conditions where Eq. (28) predicts $\sigma < 0$ are related to times during a fire scenario when the temperature of the plume at the elevation of interface penetration is predicted to be uniformly less than T_U . Under such circumstances the penetrating plume flow is nowhere positively (i.e., upward) buoyant as it enters the upper layer. Thus, while all of this flow is assumed to enter and mix with the upper layer, it is predicted above that none of it rises to the ceiling in a coherent plume, i.e., $Q'=0$. For this reason, when $\sigma < 0$ the existence of any significant ceiling jet flow is precluded along with significant convective heat transfer to the ceiling surface or to near-ceiling-deployed fusible links.

The above analysis assumes that $y_{\text{FIRE}} < y$. However, at the onset of the fire scenario $y_{\text{FIRE}} < y = y_{\text{CEIL}}$ and, since they depend on the unknown initial value of T_U , α , σ and m^* of Eqs. (27)-(29) are undefined. More critical, however, is the fact that an internally-consistent value for ρ_U is required, but not available, to initiate the solution to the governing equations. The solution to this problem will be addressed in the last section of this work. For now, we assume that we are dealing with $t > 0$, when T_U is well-known.

3.4.2. General Properties of the Plume in the Upper Layer

When the fire is below the interface, the results of Eqs. (31') and (32') allow us to describe the fire-driven plume dynamics in the upper layer according to the point source plume model of [9]. If the fire is at or above the interface, i.e., $y_{\text{FIRE}} \geq y$, then $m_{\text{PLUME}} = 0$, $q_{\text{PLUME}} = (1 - \lambda_r)Q$, and we continue to use the point source model to simulate the upper layer plume flow. All cases can be treated with the following final versions of Eqs. (31') and (32')

$$Q' = \begin{cases} (1 - \lambda_r)Q\sigma m^*/(1 + \sigma) & \text{if } y_{\text{FIRE}} < y; \\ (1 - \lambda_r)Q & \text{if } y_{\text{FIRE}} \geq y \end{cases} \quad (31')$$

$$y'_{\text{SOURCE}} = \begin{cases} y - (y - y_{\text{FIRE}})\alpha^{3/5}m^{*2/5}[(1 + \sigma)/\sigma]^{1/5} & \text{if } y_{\text{FIRE}} < y; \\ y_{\text{FIRE}} & \text{if } y_{\text{FIRE}} \geq y \end{cases} \quad (32')$$

where m^* , σ , and α are calculated from Eqs. (25)-(29).

Q' and y'_{SOURCE} of Eqs. (31') and (32') are the strength and location of a source of buoyancy embedded in the extended upper layer environment. This source is equivalent to the actual fire in the sense that Q' , y'_{SOURCE} , and the point source plume model of Reference [9] describe the dynamics of the fire plume once it enters into and passes upward through the upper layer to the ceiling. Such an upper-layer plume description is required and will be used below to predict ceiling jet-driven convective heat transfer to the ceiling surface and to vent- and sprinkler-actuating fusible links.

3.4.3. Computing q_{HT} and the Thermal Response of the Ceiling

When the fire is below the interface and the interface is below the ceiling we will use the method of [11] for calculating the heat transfer from the plume-driven ceiling jet to the ceiling and the thermal response of the ceiling.

This method was developed to treat generic, confined-ceiling, room fire scenarios. As in [11] we will solve the confined ceiling problem by applying the unconfined ceiling heat transfer solution, developed in [12] and [13], and applied in [14], to the problem of an Eq. (31')-(32') equivalent upper layer source in an extended upper layer environment. When the fire is above the interface, the unconfined ceiling methodology applies directly.

To use the methods of [11]-[14] we consider an arbitrary instant of time during the course of fire development. We assume that the temperature distribution of the ceiling material, T , has been computed up to this time and is known as a function of distance, Z , measured upward from the bottom surface of the ceiling, and radial distance, r , measured from the constant point of plume-ceiling impingement. Then the equivalent, extended-upper-layer, unconfined-ceiling flow and heat transfer problem is depicted in Figure 2. It involves the equivalent Q' heat source of Eq. (31') located a distance H below the ceiling surface in an extended ambient environment of density ρ_U and absolute temperature T_U , where H is found from Eqs. (30) and (32).

The objective here is to estimate the instantaneous convective heat transfer flux from the upper-layer gas to the lower ceiling surface, $q''_{CONV,L}(r,t)$, and the net heat transfer fluxes to the upper and lower surface of the ceiling, $q''_U(r,t)$ and $q''_L(r,t)$, respectively. With this information, the time-dependent solution for the indepth thermal response of the ceiling material can be advanced to subsequent times. Also, $q''_{CONV,L}$ can be integrated over the lower ceiling surface to obtain the desired instantaneous value for q_{HT} .

In view of assumptions in Section 3.3 on the relatively large distance of the fire from walls or curtains and on the relatively small contribution of heat transfer to these vertical surfaces, it is reasonable to carry out a somewhat simplified calculation for q_{HT} . Thus, q_{HT} will be approximated by the integral of $q''_{CONV,L}$ over an effective circular ceiling area A_{EFF} with diameter D_{EFF} , centered at the point of impingement.

$$q_{HT} = -\lambda_{CONV}Q(t) = -\int_A q''_{CONV,L}(r,t)dA \approx -2\pi \int_0^{D_{EFF}/2} q''_{CONV,L}(r,t)rdr \quad (33)$$

The value $A_{EFF} = \pi D_{EFF}^2/4$ will be taken to be the actual area of the curtained space, A , plus the portion of the vertical curtain and wall surfaces estimated to be covered by ceiling jet-driven wall flows. An estimate for this extended, effective ceiling surface area is obtained in [15] where it is concluded with some generality that ceiling jet-driven wall flows will penetrate a distance of approximately $0.8H$ down from the ceiling. Thus

$$A_{EFF} = \pi D_{EFF}^2/4 = A + 0.8H(P - L_{CURT}) + L_{CURT} \min[0.8H, (y_{CEIL} - y_{CURT})] \quad (34)$$

where P is the total length of the perimeter of the curtained area.

3.4.3.1. Net Heat Transfer Flux to the Ceiling's Lower Surface

The net heat transfer flux to the ceiling's lower surface, q_L'' , is made up of three components, incident radiation, $q_{\text{RAD-FIRE}}''$, convection, $q_{\text{CONV,L}}''$, and reradiation, $q_{\text{RERAD,L}}''$

$$q_L'' = q_{\text{RAD-FIRE}}'' + q_{\text{CONV,L}}'' + q_{\text{RERAD,L}}'' \quad (35)$$

As discussed below in Section 3.2 the radiant energy from the fire, $\lambda_r Q$, is assumed to be radiated isotropically from the fire with negligible radiation absorption and emission from the compartment gases. Therefore

$$q_{\text{RAD-FIRE}}'' = \{ \lambda_r Q / [4\pi(y_{\text{CEIL}} - y_{\text{FIRE}})^2] \} \{ 1 + [r / (y_{\text{CEIL}} - y_{\text{FIRE}})]^2 \}^{-3/2} \quad (36)$$

The convective heat transfer flux from the upper-layer gas to the ceiling's lower surface can be calculated from [12,13]

$$q_{\text{CONV,L}}'' = h_L (T_{\text{AD}} - T_{\text{S,L}}) \quad (37)$$

where $T_{\text{S,L}}$ is the absolute temperature of the ceiling's lower surface, T_{AD} , a characteristic gas temperature, is the temperature that would be measured adjacent to an adiabatic lower ceiling surface, and h_L is a heat transfer coefficient. h_L and T_{AD} are given by

$$h_L/h = \begin{cases} 8.82 \text{Re}_H^{-1/2} \text{Pr}^{-2/3} [1 - (5.0 - 0.284 \text{Re}_H^{0.2})(r/H)] & \text{if } 0 \leq r/H < 0.2; \\ 0.283 \text{Re}_H^{-0.3} \text{Pr}^{-2/3} (r/H)^{-1.2} (r/H - 0.0771) / (r/H + 0.279) & \text{if } 0.2 \leq r/H \end{cases} \quad (38)$$

$$(T_{\text{AD}} - T_U) / (T_U Q_H^{*2/3}) = \begin{cases} 10.22 - 14.9r/H & \text{if } 0 \leq r/H < 0.2; \\ 8.39f(r/H) & \text{if } 0.2 \leq r/H \end{cases} \quad (39)$$

where

$$f(r/H) = [1 - 1.10(r/H)^{0.8} + 0.808(r/H)^{1.6}] / [1 - 1.10(r/H)^{0.8} + 2.20(r/H)^{1.6} + 0.690(r/H)^{2.4}] \quad (40)$$

$$\begin{aligned} h &= \rho_U C_p g^{1/2} Q_H^{*1/3}; \\ Re_H &= g^{1/2} H^{3/2} Q_H^{*1/3} / \nu_U; \\ Q_H^* &= Q' / [\rho_U C_p T_U (gH)^{1/2} H^2] \end{aligned} \quad (41)$$

In the above, Pr is the Prandtl number (taken to be 0.7) and ν_U is the kinematic viscosity of the upper layer gas which is assumed to have the properties of air. Also, Q_H^* , a dimensionless number, is a measure of the strength of the plume and Re_H is a characteristic Reynolds number of the plume at the elevation of the ceiling.

The following estimate for ν_U of air [16] will be used when computing Re_H from Eqs. (41)

$$\nu_U / (m^2/s) = [0.04128(T_U/K)^{5/2} 10^{-7}] / [(T_U/K) + 110.4] \quad (42)$$

As the fire simulation proceeds, the ceiling's lower surface temperature, $T_{S,L}$, initially at T_{AMB} , begins to increase. At all times the lower ceiling surface is assumed to radiate diffusely to the initially ambient-temperature floor surface and to exposed surfaces of the building contents. In response to this radiation, and to the direct radiation from the fire's combustion zone, the temperature of these surfaces also increase with time. However, for times of interest here it is assumed that the effective temperature increase of these floor/contents surfaces are relatively small compared to the characteristic increases of $T_{S,L}$. Accordingly, at a given radial position of the ceiling's lower surface, the net radiation exchange between the ceiling and the floor/contents surfaces can be approximated by

$$q_{RERAD,L}'' = \sigma(T_{AMB}^4 - T_{S,L}^4) / (1/\epsilon_L + 1/\epsilon_{FLOOR} - 1) \quad (43)$$

where σ is the Stefan-Boltzmann constant and ϵ_L and ϵ_{FLOOR} are the effective emittance/absorptance of the assumed-grey ceiling upper surface and floor/contents surfaces, respectively, both of which will be taken to be 1.

3.4.3.2. Net Heat Transfer Flux to Ceiling's Upper Surface

It is assumed that the ceiling's upper surface is exposed to a relatively constant-temperature far-field environment at temperature T_{AMB} . Then the net heat transfer flux to this surface, q_L'' , is made up of two components,

convection, $q''_{CONV,U}$, and reradiation, $q''_{RERAD,U}$

$$q''_U = q''_{CONV,U} + q''_{RERAD,U} \quad (44)$$

These can be estimated from

$$q''_{CONV,U} = h_U(T_{AMB} - T_{S,U}) \quad (45)$$

$$q''_{RERAD,U} = \sigma(T_{AMB}^4 - T_{S,U}^4)/(1/\epsilon_U + 1/\epsilon_{FAR} - 1) \quad (46)$$

where $T_{S,U}$ is the absolute temperature of the upper surface of the ceiling, h_U is a heat transfer coefficient, and ϵ_{FAR} and ϵ_U are the effective emittance/absorptance of the assumed-grey far-field and ceiling upper surface, respectively, both of which will be taken to be 1.

The value for h_U to be used here is [17]

$$h_U/(W/m^2) = 1.675 |(T_{AMB}/K) - (T_{S,U}/K)|^{1/3} \quad (47)$$

3.4.3.3. Solving for the Thermal Response of the Ceiling and for q_{HT}

The temperature of the ceiling material is assumed to be governed by the Fourier heat conduction equation. By way of the lower ceiling surface boundary condition, the boundary value problem is coupled to, and must be solved together with the system of Eqns (6) and (7').

Initially the ceiling is taken to be of uniform temperature, T_{AMB} . The upper and lower ceiling surfaces are then exposed to the radial- and time-dependent rates of heat transfer q''_U and q''_L , determined from Eqs. (44) and (35), respectively. For times of interest here, radial gradients of q''_U and q''_L are assumed to be small enough so that conduction in the ceiling is quasi-one-dimensional in space, i.e., $T=T(Z,t;r)$. Thus, the two-dimensional thermal response for the ceiling can be obtained from the solution to a set of one-dimensional conduction problems for $T_n(Z,t)=T(Z,t;r=r_n)$, $n=1$ to $NRAD$, where $NRAD$ is the number of discrete radial position required to obtain a sufficiently smooth representation of the overall ceiling temperature distribution.

The parametric study of [14] for the thermal response of unconfined ceilings above constant and growing fires indicates generally that changes in T occur smoothly over the radial distances of order one when scaled by H , i.e., $d(T/T_{MAX})/d(r/H)=O(1)$, where $T_{MAX}(t)=T_{S,L}(r=0,t)=T(Z=0,t;r=0)$. Thus, it is reasonable to expect accurate results for the Eq. (33) integral of the

$q''_{CONV,L}$ distribution, which depends on the radial distribution of $T_{S,L}(r,t)=T(Z=0,t;r)$ through Eq. (37), by carrying out the following procedure: Choose NRAD as several times $D_{EFF}/[2(y_{CEIL} - y_{FIRE})]$, where the latter value is assumed to be > 0.2 (here we choose NRAD as the first integer equal to or greater than $5D_{EFF}/[2(y_{CEIL} - y_{FIRE})]+2$); place one node point at $r = 0$ and distribute with uniform separation the remaining NRAD radial node points at and between $r = 0.2(y_{CEIL} - y_{FIRE})$ and $r = D_{EFF}/2$; solve for the NRAD temperature distributions T_n and use the lower surface values of these, the $T_{S,L,n}(t)=T_{S,L}(r=r_n,t)=T_n(Z=0,t;r=r_n)$, to compute the corresponding discrete values of $q''_{CONV,L,n}(t)=q''_{CONV,L}(r=r_n,t)$ from Eq. (37); approximate the $q''_{CONV,L}$ distribution in r by interpolating between the $q''_{CONV,L,n}$ (here we will use linear interpolation); and carry out the integration indicated in Eq. (33).

The procedure for solving for the T_n is the same as that used in [14]. It requires the thickness, thermal conductivity and thermal diffusivity of the ceiling material. The solution to the one-dimensional heat conduction equation involves an explicit finite difference scheme which uses the algorithm taken from [18,19]. For a given set of calculations, $N \leq 20$ equal-spaced nodes are positioned at the surfaces and through the thickness of the ceiling at every radius position r_n . The spacing, δZ , of these is selected to be large enough (based on a maximum time step) to insure stability of the calculation.

4. Actuation of Vents and Sprinklers by Near-Ceiling-Deployed Fusible Links

It is an objective of this work to simulate conditions in building spaces where ceiling vents and sprinkler links can be actuated by the responses of near-ceiling-deployed fusible links. The idea is that during the course of a compartment fire a deployed link will be engulfed by the near-ceiling convective flow of the elevated-temperature products of combustion and entrained air of the fire-generated plume. As the fire continues, convective heating of the link will lead to an increase in its temperature. If and when its fuse temperature is reached, the device(s) being operated by the link will be actuated.

The near-ceiling flow engulfing the link is the plume-driven ceiling jet, referred to earlier, which transfers heat to the lower ceiling surface and is cooled as it traverses under the ceiling from the point of plume-ceiling impingement. In the case of relatively smooth-ceiling configurations, assumed to be representative of the facilities studied in this work, the ceiling jet flows outward radially from this point of impingement and its gas velocity and temperature distributions, V_{CJ} and T_{CJ} , respectively, are a function of radius from the impingement point, r , distance below the ceiling, z , and time.

4.1 Predicting the Thermal Response of the Fusible Links

We calculate the thermal response of deployed fusible links, up to their fuse temperature, T_F , by the convective heating flow model developed in [20]. We

assume that a link of interest is positioned at a specified radius from the impingement point, $r = r_L$, and distance below the lower ceiling surface, $z = z_L$. We define T_L as the link's assumed-near-uniform temperature. Then instantaneous changes in T_L are determined by

$$dT_L/dt = (T_{CJ,L} - T_L)V_{CJ,L}^{1/2}/RTI \quad (48)$$

where $T_{CJ,L}$ and $V_{CJ,L}$ are the values of T_{CJ} and V_{CJ} , respectively, evaluated local to the link position and where RTI (Response Time Index), a property of the link and relative flow orientation, can be measured in the "plunge test" described in [20, 21]. RTI's for ordinary sprinkler links range from a low values of $22(m \cdot s)^{1/2}$ for quick operating residential sprinklers, to $375(m \cdot s)^{1/2}$ for slower standard sprinklers [22]. The utility of Eq. (48), which is shown in [23] to be valid typically through the link fusing process, is discussed further in [22] and actually used there to predict link response in a parametric study involving two-layer compartment fire scenarios. Also, the link response prediction methodology of the latter study was used in the work of reference [22] which reports favorable comparisons between predicted and measured link responses in a full-scale, one-room, open-doorway compartment fire experiment.

To compute T_L from Eq. (48) for a different link locations requires estimates of $V_{CJ,L}$ and $T_{CJ,L}$ for arbitrary link position, r_L and z_L .

4.2 The Velocity Distribution of the Ceiling Jet

Outside of the plume/ceiling impingement stagnation zone, defined approximately by $r/H \geq 0.2$, and at a given r , V_{CJ} rises rapidly from zero at the ceiling's lower surface, $z=0$, to a maximum, V_{MAX} , at a distance $z=0.23\delta$, $\delta(r)$ being the distance below the ceiling where $V/V_{MAX}=1/2$ [15]. In this region outside the stagnation zone, V_{CJ} can be estimated from [15]

when $r/H \geq 0.2$:

$$V_{CJ}/V_{MAX} = \begin{cases} (8/7)[z/(0.23\delta)]^{1/7}(1 - [z/(0.23\delta)]/8), & 0 \leq z/(0.23\delta) \leq 1 \\ \cosh^{-2}\{(0.23/0.77)\operatorname{arccosh}(2^{1/2})[z/(0.23\delta) - 1]\}, & 1 \leq z/(0.23\delta) \end{cases} \quad (49)$$

$$V_{MAX}/V = 0.85(r/H)^{-1.1} ; \delta/H = 0.10(r/H)^{0.9} ; V = g^{1/2}H^{1/2}Q_H^*{}^{1/3} \quad (50)$$

where Q_H^* is defined in Eq. (41). V_{CJ}/V_{MAX} per Eq. (49) is plotted in Figure 3.

In the vicinity of near-ceiling-deployed links located inside the stagnation zone, the fire-driven flow is changing directions from an upward-directed plume flow to a outward-directed ceiling-jet-type flow. There the flow velocity local to the link, the velocity which drives the link's convective heat transfer, involves generally a significant vertical as well as radial component of velocity. Nevertheless, at such link locations it is reasonable to continue to approximate the link response by Eq. (48) with V_{CJ} estimated by Eqs. (49) and (50) and with r/H is set equal to 0.2, i.e.,

when $0 \leq r/H < 0.2$

$$V_{CJ} = V_{CJ}(r/H = 0.2) \quad (51)$$

This approximation is adopted here.

4.3 The Temperature Distribution of the Ceiling Jet

Outside of the plume-ceiling impingement stagnation zone, i.e., where $r/H \geq 0.2$, and at a given value of r , T_{CJ} rises very rapidly from the temperature of the ceiling's lower surface $T_{S,L}$, at $z=0$, to a maximum, T_{MAX} , somewhat below the ceiling surface. We assume that this maximum value of T_{CJ} occurs at the identical distance below the ceiling as does the maximum of V_{CJ} , i.e., at $z=0.23\delta$. Below this elevation, T_{CJ} drops with increasing distance from the ceiling until it reaches the upper layer temperature, T_U . In this latter, outer region of the ceiling jet, the shape of the normalized T_{CJ} distribution, $(T_{CJ}-T_U)/(T_{MAX}-T_U)$, will have the same characteristics as does that of V_{CJ}/V_{MAX} . Also, since we are dealing with a turbulent boundary flow it is reasonable to expect that the characteristic thicknesses of the outer region of both the velocity and temperature distributions are the same, being dictated there by the distribution of the turbulent eddies.

For the above reasons we approximate the velocity and temperature distributions as being identical in the outer region of the ceiling jet flow, $0.23\delta \leq z$. In the inner region of the flow, between $z=0$ and 0.23δ , we approximate the normalized temperature distribution by a quadratic function of $z/(0.23\delta)$, requiring $T_{CJ}=T_{S,L}$ at $z=0$ and $T_{CJ}=T_{MAX}$, $dT_{CJ}/dz=0$ at $z=0.23\delta$. Thus,

when $r/H \geq 0.2$:

$$\theta \equiv (T_{CJ} - T_U) / (T_{MAX} - T_U) = \begin{cases} \theta_s + 2(1 - \theta_s)[z/(0.23\delta)] - (1 - \theta_s)[z/(0.23\delta)]^2, & 0 \leq z/(0.23\delta) \leq 1 \\ V_{CJ}/V_{MAX}, & 1 \leq z/(0.23\delta) \end{cases} \quad (52)$$

$$\theta_s \equiv \theta(T_{CJ}=T_{S,L}) = (T_{S,L} - T_U) / (T_{MAX} - T_U) \quad (53)$$

Note that θ_s will be negative when the ceiling surface temperature is less than the upper layer temperature, for example, relatively early in the fire when the original ambient-temperature ceiling surface has not yet reached the average temperature of the growing upper layer. Also, θ_s will be greater than 1 when the ceiling surface temperature is greater than T_{MAX} . This is possible, for example, during times of reduced fire size when the fire's near-ceiling plume temperature is reduced significantly, perhaps temporarily, from previous values, but the ceiling surface, heated previously to relatively high temperatures, has not cooled substantially. Plots of θ per Eq. (52) are presented in Figure 4 for cases when θ_s is <0 , between 0 and 1, and >0 .

In a manner similar to the treatment of V_{CJ}/V_{MAX} , for the purpose of calculating T_L from Eq. (48) we approximate θ_s inside the stagnation zone by the description of Eqs. (52) and (53) with r/H set equal to 0.2, i.e.,

when $0 \leq r/H \leq 0.2$:

$$\theta_s = \theta_s(r/H = 0.2) \quad (54)$$

With the radial distribution for $T_{S,L}$ and T_U already calculated up to a particular time of interest, only T_{MAX} is required to complete the Eqs. (52)-(54) estimate for the ceiling jet temperature distribution. This is obtained by invoking conservation of energy. Thus, at an arbitrary r outside the stagnation zone the total rate of radial outflow of enthalpy (relative to the upper layer temperature) of the ceiling jet is equal to the uniform rate of enthalpy flow in the upper layer portion of the plume, Q' , less the integral (from the plume-ceiling impingement point to r) of the flux of convective heat transfer from the ceiling jet to the ceiling surface, i.e.,

when $0.2 \leq r/H$:

$$2\pi \int_0^{\infty} \rho_U C_p (T_{CJ} - T_U) V_{CJ} z dz = Q' - 2\pi \int_0^r q''_{CONV,L}(r,t) r dr \equiv (1 - \lambda'_{CONV}) Q' \quad (55)$$

λ'_{CONV} is the fraction of Q' transferred by convection to the ceiling from the point of ceiling impingement to r , i.e.,

$$\lambda'_{CONV}(r) = [2\pi \int_0^r q''_{CONV,L}(r,t) r dr] / Q' \quad (56)$$

In Eqs. (55) and (56), Q' has been calculated previously in Eqs. (41). Also, the integral on the right hand sides of Eqs. (55) and (56) can be calculated by approximating $q''_{CONV,L}(r,t)$, as discussed above in section 3.4.3.3, as a linear function of r between previously calculated values of $q''_{CONV,L}(r=r_n, t)$.

The integral on the left hand side of Eq. (55) is calculated using V_{CJ} of Eqs. (49) and (50) and T_{CJ} of Eqs. (52) and (53). From this the desired distribution for T_{MAX} is found finally to be

$$(T_{MAX} - T_U) = 2.6(1 - \lambda'_{CONV})(r/H)^{-0.8} Q_H^{*2/3} T_U - 0.090(T_S - T_U), \quad 0.2 \leq r/H \quad (57)$$

The above result together with Eqs. (52) and (53) represent the desired estimate for T_{CJ} . This and the Eqs. (49)-(51) estimate for V_{CJ} are used to calculate T_L from Eq. (48).

4.4 Dependence of Open Vent Area on Fusible Link-Actuated Vents

As discussed above in section 3.1, the influence of ceiling vent action on the fire-generated environment is dependent on the active area of the open ceiling vents, A_v . A variety of basic vent opening design strategies are possible and it is a major purpose of this work to evaluate these within the context of the developing fire environment. For example, one of the simplest strategies, the one examined in reference [1], assumes that all vents deployed in the curtained area of interest are opened by whatever means at the onset of the fire. In general A_v will be time-dependent. To the extent that a strategy of vent opening is dependent directly on the fusing of any one or several deployed fusible links, the location of these links and their characteristics (i.e., likely spacings from plume-ceiling impingement, distance below the ceiling, and the RTI) and the functional relation between link fusing and A_v must be specified. These matters, to be examined in the context of different solutions to the overall problem, will be addressed in [2].

5. Initiating the Solution of the Model Equations

The basic independent variables describing the fire-generated environment are y and ρ_U . These are determined from the solution to Eqs. (6) and (7'), respectively. The right hand sides of these latter equations depend on the time-dependent values of m_U and q_U which are computed from Eqs. (4) and (5), respectively, through use of the variety of algorithms described in this work.

The solution to the governing equations requires the initial value of y and ρ_U . The first of these is specified to be y_{CEIL} . The second must be determined from Eq. (8). But this calls for initial values for m_U and q_U which are not available. Therefore, the determination of $\rho_U(t=0)$ requires the special considerations described below.

m_U and q_U are determined by evaluating the individual terms on the right hand sides of Eqs. (4) and (5) as follows.

Since $y - y_{CEIL} = 0$, $m_{VENT} = 0$ from Eq. (12) and $q_{VENT} = 0$ from Eq. (13). Since $y_{CURT} - y < 0$, $m_{CURT} = 0$ from Eq. (20) and $q_{CURT} = 0$ from Eq. (21).

From the initial characteristics of the fire, $Q > 0$, y_{FIRE} , and D_{FIRE} , compute L_{FLAME} from Eq. (17). Using this, calculate $(y - y_{FIRE}) / L_{FLAME}$. Determine m_{PLUME} from Eq. (16), m_{ENT} from Eq. (14), and then $q_{PLUME} = m_{ENT} C_p T_{AMB} + (1 - \lambda_r) Q$ from Eq. (15).

At this stage of the calculation, use of Eqs. (8) and (3) together with the above results leads to the following equation for the unknown $T_U(t=0)$

$$T_U(t = 0) - [m_{ENT} C_p T_{AMB} + (1 - \lambda_r) Q + q_{HT}] / (m_{ENT} C_v) = 0 \quad (58)$$

Except for $T_U(t=0)$, q_{HT} is the only remaining unknown in Eq. (58). Furthermore, at time $t=0$ of interest q_{HT} is a function of $T_U(t=0)$, i.e., $q_{HT} = f(T_U)$. Since q_{HT} is in the range

$$-(1 - \lambda_r) Q < q_{HT} < 0 \quad (59)$$

it follows that the unknown $T_U(t=0)$ is the presumably unique root of Eq. (58) which lies within the range

$$T_{AMB} < T_U(t = 0) < [m_{ENT} C_p T_{AMB} + (1 - \lambda_r) Q] / (m_{ENT} C_v)$$

The functional relationship between q_{HT} and $T_U(t=0)$ is determined from Eqs. (25)-(34) and (37)-(42) where $T_{S,L} = T_{AMB}$ in Eq. (37). Thus, for each node point at $r=r_n$ on the lower ceiling surface, $q_{CONV,L,n}(t=0)$ is computed from

Eq. (37) and, as discussed in the third paragraph of section 3.4.3.3, q_{HT} is obtained finally from Eq. (33).

6. Concluding Remarks

The theory presented here is the basis of a computer model now under development. This will be used to study parametrically a wide range of relevant fire scenarios. The results of the parametric study will be presented in Part II of this work [2]: Estimating the Environment and the Response of Sprinkler Links in Compartment Fires with Draft Curtains and Fusible Link-Actuated Ceiling Vents - Part II: Application (tentative title).

7. Acknowledgements

The author acknowledges gratefully the AAMA Research Foundation which supported this work.

8. References

- [1]. Hinkley, P.L., The Effect of Vents on the Opening of the First Sprinklers, *Fire Safety Journal*, 11, pp. 211-225, 1986.
- [2]. Walton, D.W., Cooper, L.Y., and Stroup, D.W., Estimating the Environment and the Response of Sprinkler Links in Compartment Fires with Draft Curtains and Fusible Link-Actuated Ceiling Vents - Part II: Application (tentative title), to be published.
- [3]. Emmons, H.W., The Flow of Gases Through Vents, Harvard University Home Fire Project Technical Report No. 75, March 16, 1987.
- [4]. Thomas, P.H., et al, Investigations Into the Flow of Hot Gases in Roof Venting, *Fire Research Technical Paper No. 7*, HMSO, London, 1963.
- [5]. Heskestad, G., Smoke Movement and Venting, *Fire Safety Journal*, 11, pp77-83, 1986, and Appendix A: Guide for Heat and Smoke Venting, NFPA 204M, National Fire Protection Association, Quincy, MA, 1982.
- [6]. Cooper, L.Y., A Mathematical Model for Estimating Available Safe Egress Time in Fires, *Fire and Materials*, 6, 3/4, pp. 135-144, 1982.
- [7]. Heskestad, G., Engineering Relations for Fire Plumes, *Fire Safety Journal*, 7, pp. 25-32, 1984.
- [8]. Hinkley, P.L., Rates of 'Production' of Hot Gases in Roof Venting Experiments, *Fire Safety Journal*, 10, pp. 57-65, 1986.
- [9]. Zukoski, e.e., Kubota, T., and Cetegen, B., *Fire Safety Journal*, 3, p 107, 1981.
- [10]. Cooper, L.Y., A Buoyant Source in the Lower of Two, Homogeneous, Stably Stratified Layers, 20th International Symposium on Combustion, Combustion Institute, pp. 1567-1573, 1984.
- [11]. Cooper, L.Y., Convective Heat Transfer to Ceilings Above Enclosure Fires, Cooper, L.Y., 19th Symposium (International) on Combustion, Combustion Institute, pp. 933-939 (1982).
- [12]. Cooper, L.Y., Heat Transfer From a Buoyant Plume to an Unconfined Ceiling, *Journal of Heat Transfer*, Vol. 104, pp. 446-451, Aug. 1982.
- [13]. Cooper, L.Y. and Woodhouse, A., The Buoyant Plume-Driven Adiabatic Ceiling Temperature Revisited, *Journal of Heat Transfer*, Vol. 108, pp. 822-826, Nov., 1986.
- [14]. Cooper, L.Y., and Stroup, D.W., Thermal Response of Unconfined Ceilings Above Growing Fires and the Importance of Convective Heat Transfer, *Journal of Heat Transfer*, Vol. 109, pp. 172-178, Feb. 1987.

- [15]. Cooper, L.Y., Ceiling Jet-Driven Wall Flows in Compartment Fires, NBSIR 87-3535, National Bureau of Standards, Gaithersburg, MD, April, 1987.
- [16]. Hilsenrath, J., Tables of Thermal Properties of Gases, Circular 564, National Bureau of Standards, Gaithersburg, MD, Nov. 1955.
- [17]. Yousef, W.W., Tarasuk, J.D., and McKeen, W.J., Free Convection Heat Transfer From Upward-Facing, Isothermal, Horizontal Surfaces, Journal of Heat Transfer, Vol. 104, pp. 493-499, Aug. 1982.
- [18]. Emmons, H.W., The Prediction of Fire in Buildings, 17th Symposium (International) on Combustion, Combustion Institute, pp. 1101-1111 (1979).
- [19]. Mitler, H.E., and Emmons, H.W., Documentation for the Fifth Harvard Computer Fire Code, Home Fire Project Tech. Report 45, Harvard University, Cambridge, MA. 1981.
- [20]. Heskestad, G. and Smith, H.F., Investigation of a New Sprinkler Sensitivity Approval Test: The Plunge Test, Technical Report Serial No. 22485, RC 76-T-50, Factory Mutual Research Corporation, Norwood, MA, 1976.
- [21]. Heskestad, G., The Sprinkler Response Time Index (RTI), Paper RC-81-TP-3 presented at the Technical Conference on Residential Sprinkler Systems, Factory Mutual Research Corporation, Norwood, MA, April 28-29, 1981.
- [22]. Evans, D.D., Calculating Sprinkler Actuation Times in Compartments, Fire Safety Journal, 9, pp 147-155, 1985.
- [23]. Evans, D.D., Characterizing the Thermal Response of Fusible Link Sprinklers, NBSIR 81-2329, National Bureau of Standards, Gaithersburg, MD, 1981.
- [24]. Cooper, L.Y. and Stroup, D.W., Test Results and Predictions for the Response of Near-Ceiling Sprinkler Links in Full-Scale Compartment Fires, NBSIR 87-3663, National Bureau of Standards, Gaithersburg, MD, 1987, to be presented at the 2nd International Symposium on Fire Safety Science, Tokyo, June, 1988 and published in the Symposium Proceedings.

9. Nomenclature

A	plan area of single curtained space
A_{EFF}	effective area for heat transfer to the extended lower ceiling surface, $\pi D_{EFF}^2/4$
A_V	total vent area of curtained space
C	vent flow coefficient (≈ 0.68)
C_p	specific heat at constant pressure
C_T	9.115, dimensionless constant in plume model
C_v	specific heat at constant volume, C_p/γ
D_{EFF}	effective diameter of A_{EFF}
D_{FIRE}	effective diameter of fire source ($\pi D_{FIRE}^2/4 =$ area of fire source)
g	acceleration of gravity
H	distance below ceiling of equivalent source
h	characteristic heat transfer coefficient
h_L, h_U	lower, upper ceiling surface heat transfer coefficient
L_{FLAME}	flame length
m^*	fraction of m_{PLUME} which is buoyant relative to T_U
m_{CURT}	mass flow rate from below curtain to upper layer
m_{ENT}	rate of plume mass entrainment between fire and layer interface
m_{PLUME}	mass flow rate of plume at interface
m_U	net mass flow rate to upper layer
m_{VENT}	mass flow rate through ceiling vents to upper layer
N	number of equal-spaced nodes through the ceiling
NRAD	number of values of r_n
P	length of perimeter of single curtained area

Pr	Prandtl number, taken to be 0.7
P	P_{AMB} at floor elevation
P_U, P_{AMB}	pressure in upper layer, outside ambient
Q	energy release rate of fire
Q'	strength of continuation source in extended upper layer
Q_H^*	dimensionless strength of plume at ceiling
Q_{EQ}^*	dimensionless strength of plume at interface
$q''_{CONV,L}, q''_{CONV,U}$	convective heat transfer flux to lower, upper ceiling surface
q_{CURT}	enthalpy flow rate from below curtain to upper layer
q_{HT}	heat transfer rate to upper layer
q_{PLUME}	enthalpy flow rate of plume at interface
$q''_{RAD-FIRE}$	radiation flux incident on lower surface of ceiling
$q''_{RERAD,L}, q''_{RERAD,U}$	reradiation flux to lower, upper surface of ceiling
q_U	net enthalpy flow rate plus heat transfer rate to upper layer
q''_L, q''_U	net heat transfer fluxes to upper, lower ceiling surface
q_{VENT}	enthalpy flow rate through ceiling vent to upper layer
$q''_{CONV,L,n}$	$q''_{CONV,L}(r=r_n, t)$
R	gas constant, $(\gamma-1)C_p/\gamma = C_p - C_v$
Re_H	Reynolds number of plume at ceiling elevation
RTI	Response Time Index
r	radial distance from point of plume-ceiling impingement
r_L	r at link
r_n	discrete values of r
T	absolute temperature of ceiling material

T_{AD}	adiabatic lower ceiling surface temperature
T_{CJ}	temperature distribution of ceiling jet gas
$T_{CJ,L}$	T_{CJ} at link
$T_{MAX}(t)$	$T_{S,L}(r=0,t) = T(Z=0,t;r=0)$
$T_{S,L}, T_{S,U}$	absolute temperature of lower, upper ceiling surface
$T_{S,L,n}(t)$	$T_{S,L}(r = r_n,t) = T_n(Z=0,t;r=r_n)$
T_U, T_{AMB}	absolute temperature of upper layer, outside ambient
T_n	$T(Z,t;r=r_n)$
t	time
V	average flow velocity through all open vents
V_{CJ}	velocity distribution of ceiling jet gas
$V_{CJ,L}$	V_{CJ} at link
V_{MAX}	maximum value of V_{CJ} at a given r
$Y, Y_{CEIL}, Y_{CURT}, Y_{FIRE}$	elevation of smoke layer interface, ceiling, bottom of curtain, fire above floor
Y'_{SOURCE}	elevation of plume continuation point source in extended upper layer above floor
Z	distance into the ceiling, measured from bottom surface
z, z_L	distance below lower ceiling surface, z at link
α	T_U/T_{AMB}
γ	ratio of specific heats, C_p/C_v
ΔP_{CEIL}	cross-vent pressure difference
ΔP_{CURT}	cross-curtain pressure difference
δ	value of z where $V_{CJ} = V_{MAX}$
δZ	distance between nodes through the ceiling thickness
ϵ	constant, Eq. (18)

$\epsilon_L, \epsilon_U, \epsilon_{\text{FLOOR}}, \epsilon_{\text{FAR}}$	emittance/absorptance of lower, upper, floor, and far field grey surfaces, all taken to be 1
Θ	normalized, dimensionless ceiling jet temperature distribution, $(T_{\text{CJ}} - T_U) / (T_{\text{MAX}} - T_U)$
Θ_S	Θ at the lower ceiling surface, $(T_{\text{S,L}} - T_U) / (T_{\text{MAX}} - T_U)$
λ_r	fraction of Q radiated from combustion zone
λ_{CONV}	fraction of Q transferred by convection from upper layer
λ'_{CONV}	fraction of Q' transferred to the ceiling in a circle of radius r, and centered at $r = 0$, Eq. (56).
ν_U	kinematic viscosity of upper layer gas
$\rho_U, \rho_{\text{AMB}}$	density of upper layer, outside ambient
σ	dimensionless variable, Eq. (20)

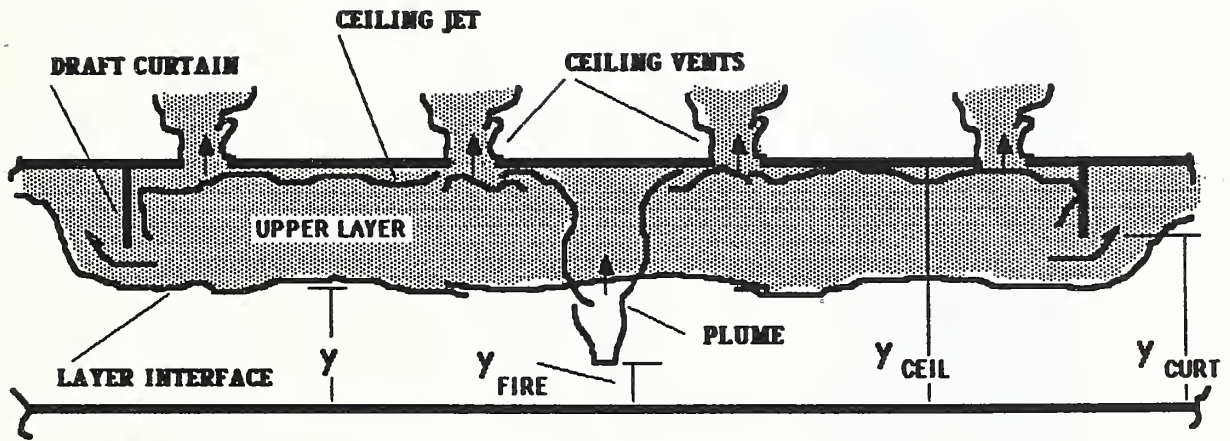


Figure 1. Fire in a building space with draft curtains and ceiling vents

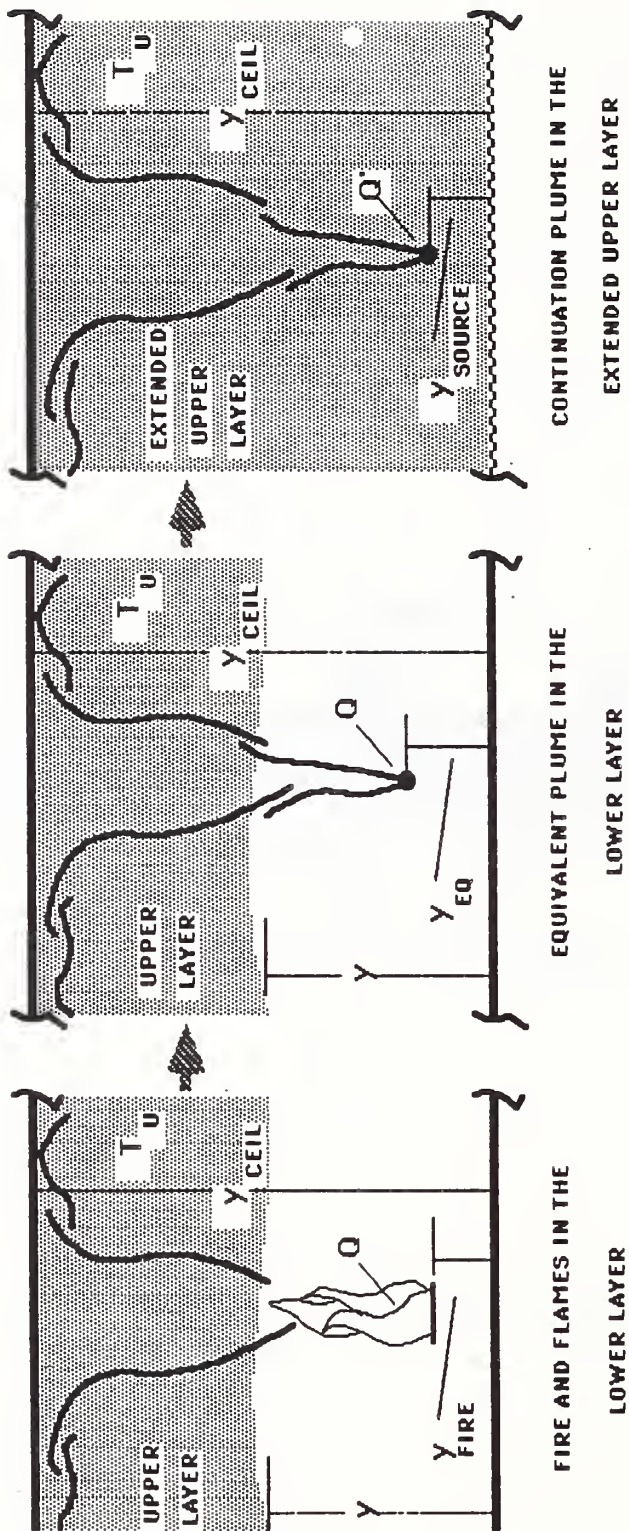


Figure 2. The fire and the equivalent source in the lower layer and the continuation source in the extended upper layer

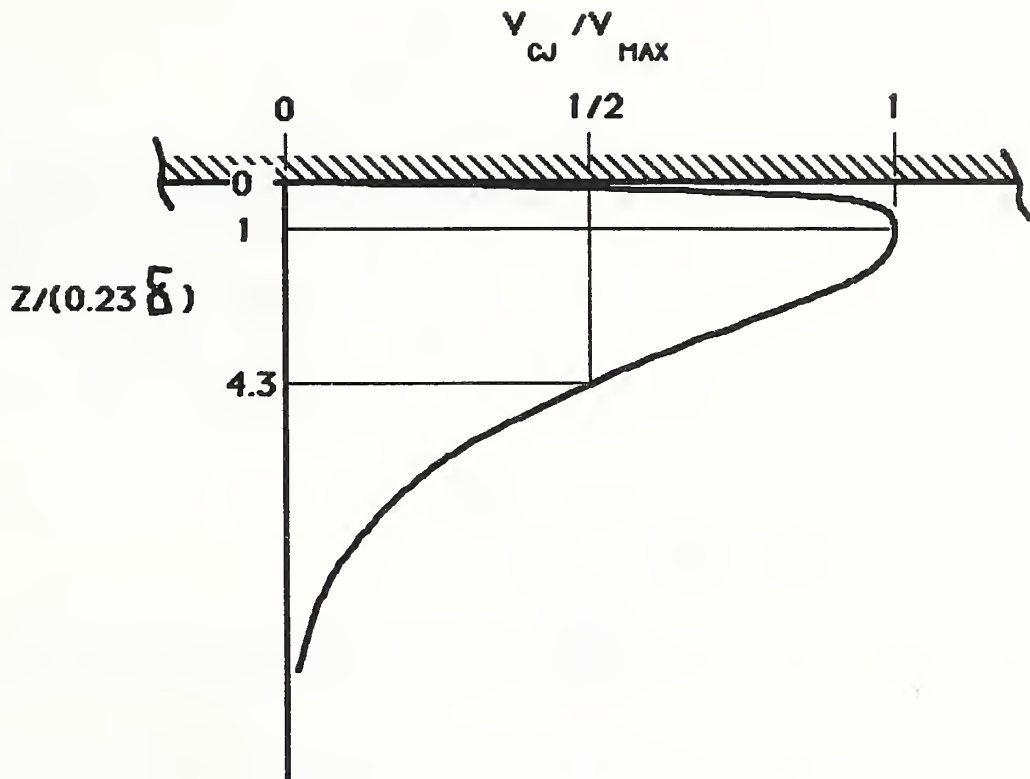


Figure 3. A plot of dimensionless ceiling jet velocity distribution, V_{CJ}/V_{MAX} , as a function of $z/(0.23\delta)$ per Eq. (49)

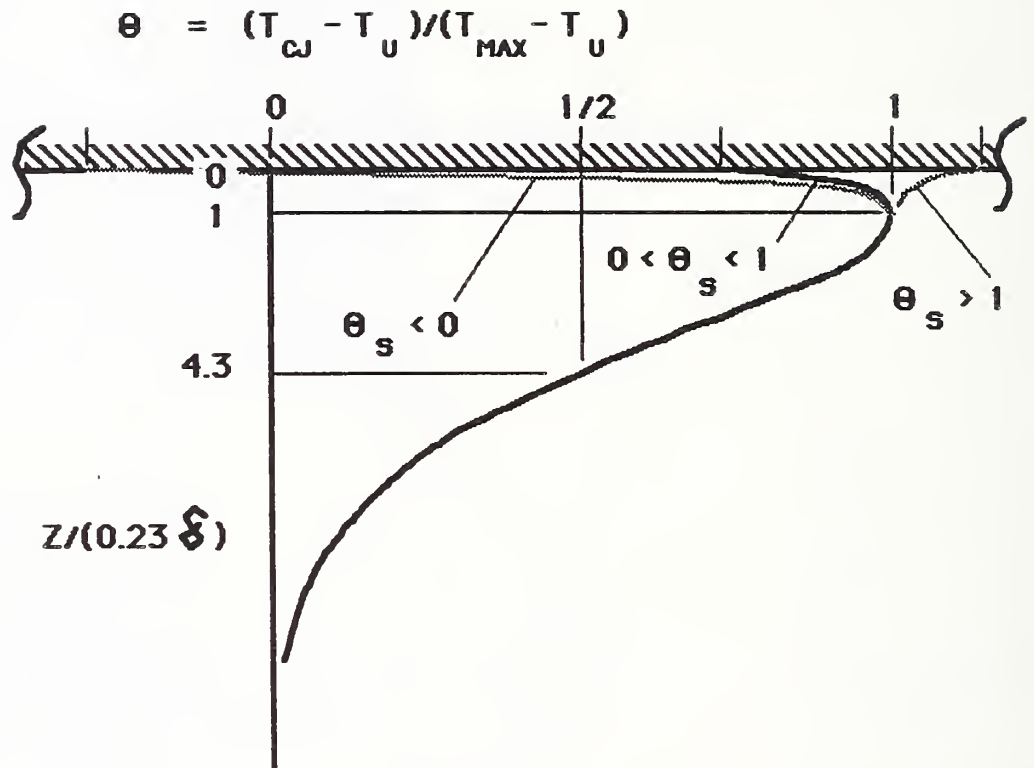


Figure 4. Plots of dimensionless ceiling jet temperature distribution, θ , as a function of $z/(0.23\delta)$ per Eq. (52) for cases when θ_s is < 0 , between 0 and 1, and > 0

U.S. DEPT. OF COMM. BIBLIOGRAPHIC DATA SHEET (See instructions)		1. PUBLICATION OR REPORT NO. NBSIR 88-3734	2. Performing Organ. Report No.	3. Publication Date April 1988
4. TITLE AND SUBTITLE Estimating the Environment and the Response of Sprinkler Links in Curtained Compartment Fires with Fusible Link-Actuated Ceiling Vents - Part I: Theory				
5. AUTHOR(S) Leonard Y. Cooper				
6. PERFORMING ORGANIZATION (If joint or other than NBS, see instructions) NATIONAL BUREAU OF STANDARDS U.S. DEPARTMENT OF COMMERCE GAITHERSBURG, MD 20899			7. Contract/Grant No.	
			8. Type of Report & Period Covered	
9. SPONSORING ORGANIZATION NAME AND COMPLETE ADDRESS (Street, City, State, ZIP) AAMA Research Foundation 2700 River Road, Suite 118 Des Plaines, Illinois 60018				
10. SUPPLEMENTARY NOTES <input type="checkbox"/> Document describes a computer program; SF-185, FIPS Software Summary, is attached.				
11. ABSTRACT (A 200-word or less factual summary of most significant information. If document includes a significant bibliography or literature survey, mention it here) The physical basis and associated mathematical model for estimating the fire-generated environment and the response of sprinkler links in well-ventilated, curtained compartment fires with fusible link-actuated ceiling vents is developed. Complete equations and assumptions are presented. Phenomena taken into account include: the flow dynamics of the upward-driven, buoyant fire plume; growth of the elevated-temperature smoke layer in the curtained compartment; the flow of smoke from the layer to the outside through open ceiling vents; the flow of smoke below curtain partitions to building spaces adjacent to the curtained space of fire origin; continuation of the fire plume in the upper layer; heat transfer to the ceiling surface and the thermal response of the ceiling as a function of radial distance from the point of plume-ceiling impingement; the velocity and temperature distribution of plume-driven near-ceiling flows and the response of near-ceiling-deployed fusible links as functions of distance below the ceiling and distance from plume-ceiling impingement. The theory presented here is the basis of a computer model now under development which will be used to study parametrically a wide range of relevant fire scenarios. The results of the parametric study will be presented in the Part II: Application portion of this paper.				
12. KEY WORDS (Six to twelve entries; alphabetical order; capitalize only proper names; and separate key words by semicolons) algorithms; building fires; compartment fires; computer models; fire models; mathematical models; vents; sprinkler response; zone models				
13. AVAILABILITY <input checked="" type="checkbox"/> Unlimited <input type="checkbox"/> For Official Distribution. Do Not Release to NTIS <input type="checkbox"/> Order From Superintendent of Documents, U.S. Government Printing Office, Washington, D.C. 20402. <input checked="" type="checkbox"/> Order From National Technical Information Service (NTIS), Springfield, VA. 22161			14. NO. OF PRINTED PAGES 37	
			15. Price \$11.95	

